



Article

Integrative Benefits of Carbon Emission and Economic Cost for Self-Healing, Ultra-Thin Overlay Contained Steel Fiber

Fusong Wang , Xiaoqing Li, Chao Huang * , Wangwang Zhou and Dongxing Luan

School of Civil and Hydraulic Engineering, Huazhong University of Science and Technology, Wuhan 430074, China; wangfs@hust.edu.cn (F.W.); xql@hust.edu.cn (X.L.); zww0210@hust.edu.cn (W.Z.)

* Correspondence: chaohuang_civil@163.com

Abstract: In recent years, self-healing, ultra-thin overlay has been recognized as an advanced technology and gradually applied in asphalt pavement maintenance, but its sustainability has not been well addressed quantitatively regarding practical maintenance projects. This study utilizes steel fiber as a media-induction material for self-healing, ultra-thin overlay and verifies its integrative benefits in terms of carbon emissions and economic costs from a six-year life-cycle perspective. The system framework and research boundary were developed to include the material extraction, on-site construction, later maintenance, and demolition phases. Meanwhile, carbon emissions and economic cost inventories were established through investigations of the test section of a maintenance project. The results indicated that self-healing, ultra-thin overlay could have benefits, with a reduction of 59.43% carbon emissions and 73.15% economic costs in the six-year life cycle, during which the material extraction phase generated over 50% of the carbon emissions and economic costs in self-healing, ultra-thin overlay due to the addition of steel fiber. Comparatively, the later maintenance phase caused the most environmental and financial impacts, with over half of the carbon emissions and costs. The obtained results could act as significant reference material for the sustainable maintenance implementation of asphalt pavement.

Keywords: asphalt pavement; steel fiber; ultra-thin overlay; self-healing; carbon emission; economic cost



Citation: Wang, F.; Li, X.; Huang, C.; Zhou, W.; Luan, D. Integrative Benefits of Carbon Emission and Economic Cost for Self-Healing, Ultra-Thin Overlay Contained Steel Fiber. *Sustainability* **2024**, *16*, 9498. <https://doi.org/10.3390/su16219498>

Academic Editor: Paulo Santos

Received: 10 September 2024

Revised: 21 October 2024

Accepted: 30 October 2024

Published: 31 October 2024



Copyright: © 2024 by the authors. Licensee MDPI, Basel, Switzerland. This article is an open access article distributed under the terms and conditions of the Creative Commons Attribution (CC BY) license (<https://creativecommons.org/licenses/by/4.0/>).

1. Introduction

Asphalt pavement maintenance has become of increasing concern in recent decades since the majority of urban road networks require preventive and corrective maintenance measures due to the manner of their construction over the years [1,2]. The Strategic Highway Research Program (SHRP) highlighted that conducting maintenance operations every three to four years would extend the service life span of asphalt pavement by 10 to 15 years and reduce the economic costs by approximately 50% [3]. According to the statistical bulletin by the Chinese Ministry of Transport, maintenance mileages already occupies 99.9% of total highway mileages, with 5.35 million kilometers in 2022 [4], reflecting the strong demand for road maintenance at present in the field of transportation infrastructure [5]. However, maintenance projects always consume massive energy resources and require high financial investments [6], resulting in significant environmental impacts and heavy financial burdens [7]. It is reported that annual investment for road maintenance works has reached CNY 600 billion in China [8]. Meanwhile, the general public have to suffer from traffic congestion [9], deteriorating air quality, and associated noise pollution around the maintenance area [10]. Generally, exploration in mitigating the negative impacts of maintenance works has become an increasingly important research topic.

The ultra-thin overlay is a widely used maintenance measure for asphalt pavement; it is thinner than other overlays [11] and is not only able to treat pavement deterioration directly but also exhibits superior improvements in skid resistance [12] and noise reduction [13]

behaviors. Moreover, several studies have confirmed that ultra-thin overlay could save a proportion of agency and user costs and reduce environmental burdens [14]. In response to the demands of low carbon emissions and sustainable development, partial modifiers and optimized approaches have been explored for ultra-thin overlay applied to asphalt pavement. Yu used basalt fiber as a partial filler to prepare the cold-mixing asphalt mixture for the ultra-thin overlay, which notably decreased the construction temperature and energy consumption [15]. Song incorporated reclaimed asphalt pavement (RAP) and glass fiber in an ultra-thin asphalt overlay, which improved fatigue life and had significant environment benefits [16]. Chen designed an ultra-thin overlay for wet-freeze climates through adding activated crumb rubber and RAP to a hot asphalt mixture, providing it with good moisture damage resistance and high sustainability [17].

Although the ultra-thin overlay is recognized as a promising alternative to asphalt pavement maintenance, extending its practical durability would currently be a challenge for further application [18]. Generally, the administrative agency would adopt extra treatments 3 to 5 years after paving the overlay [19,20], and once micro cracks and rut deformations appear on the surface of the ultra-thin overlay, it would be difficult for common corrective treatments to restore its performance due to the limited maintenance space as it has an approximate thickness of less than 25 mm [21,22]. Therefore, exploring nondestructive approaches in repairing slight deformations would be useful for preventing the deterioration of servicing properties and increase the durability of ultra-thin overlay.

Since the healing behavior of asphalt mixture was reported by Bazin and Saunier in 1967 [23], self-healing asphalt pavement by electromagnetic induction has been increasingly discussed in the field of infrastructure construction [24]. Specifically, electromagnetic induction could heat the mediums in the asphalt mixture to allow the asphalt binder movement to smooth out cracks and defects [25,26]. A majority of studies advocate the sustainability and construction simplicity of self-healing strategies for asphalt pavement [27]. Yang evaluated the multiple induction heating characteristics of asphalt mixture with steel slag and RAP [28]. Ye assessed the multiple induction heating capacity of recycled asphalt mixture by incorporating RAP and recycled concrete aggregate (RCA) [29] and improved the induction healing efficiency by adding waste carbon fibers [30]. Li used steel slag and steel fiber to obtain self-healing properties via the application of microwave heating [31]. Moreover, several studies have investigated the treatment of icy pavement by induction heating. Jiao used steel slag to produce a conductive asphalt mixture with the purpose of obtaining a thermal condition, melting the surface snow [32]. Liu claimed that electromagnetic induction could save 42.27% of energy consumption in ice melting [33].

Reducing carbon emissions has become a significant challenge for road construction and maintenance projects [34]. Several previous studies have quantified the environmental impacts of self-healing technology, aiming to verify its practical benefits when applied on asphalt pavement. Esther concluded that induction healing asphalt pavement could reduce environmental burdens by 8% over a 30-year period [35]. Ana claimed that self-healing asphalt pavement could decrease GHG emissions by 16% and costs by 32% over its entire lifecycle [36]. Liu explored the benefits of self-healing asphalt pavement via induction heating with steel slag, and their results indicated that approximately 5 tons of CO₂ emissions and USD 44,502.86 of economic costs could be saved for 1 km of a single traffic lane [37]. Wang assessed the environmental impacts of asphalt pavement in the construction period, and the results showed that 1 km of a self-healing layer would generate 139.51 tons of CO₂ emissions and 1.81 TJ of energy consumptions [38].

To overcome the limited servicing life and obtain functional effects, the employment of induction self-healing technology in ultra-thin overlay has been proposed since the thin structure could lead to rapid thermal conductive healing. Wan integrated steel slag and steel fibers into an asphalt mixture for ultra-thin overlays and investigated the self-healing efficiency [39] and ice melting capacity [40], respectively. The results indicated that a 3% addition of steel fiber could obtain the appropriate properties for both self-healing and mechanical performances. Liu analyzed the induction healing strengths of ultra-thin

overlay by mixing the asphalt binder with different ageing levels, and their results showed that the average temperature and heating rate of induction heating were significantly decreased with the aging degree of the asphalt binder [41]. Xu assessed the mechanical durability and induction healing property for porous ultra-thin overlay with steel fiber and steel slag aggregate and revealed that a temperature ranging from 100 to 120 °C would work well for the healing action [42].

Previous studies have attached importance to the induction heating efficiency and mechanical properties of self-healing, ultra-thin overlay (SH overlay), ignoring the quantification of its environmental impact and economic cost with practical pavement maintenance cases [38,43], which could hinder project managers and decision-makers in drawing up maintenance plans for asphalt pavement [44]. This study attempts to establish a research framework and basic data inventory for an integrative assessment system of self-healing, ultra-thin overlay and conducts a comparative analysis with traditional overlay (TR overlay) from case study results regarding GHG emissions and economic costs. The obtained results could provide a significant basis for maintenance decision-making and promote the implementation of sustainable road construction.

2. Materials and Methods

2.1. Materials

This study has investigated the primary data from a test section of a maintenance project in Jingyang Town, Fuqing City, Fujian Province. In the maintenance area, most of the driving vehicles are cars or small cargo vehicles, with a designed speed of 40 km/h, and the test section was paved with a self-healing, ultra-thin overlay with a thickness of 20 mm and a width of 9 m. Figure 1 shows the maintenance area of the self-healing, ultra-thin overlay. It is noted that the experimental results have already verified the practicability and self-healing performance of self-healing asphalt mixtures before paving the test section, whose induction heating rate could reach 3.0 °C/s, with a steel fiber content of 2.4% of mineral materials mass.

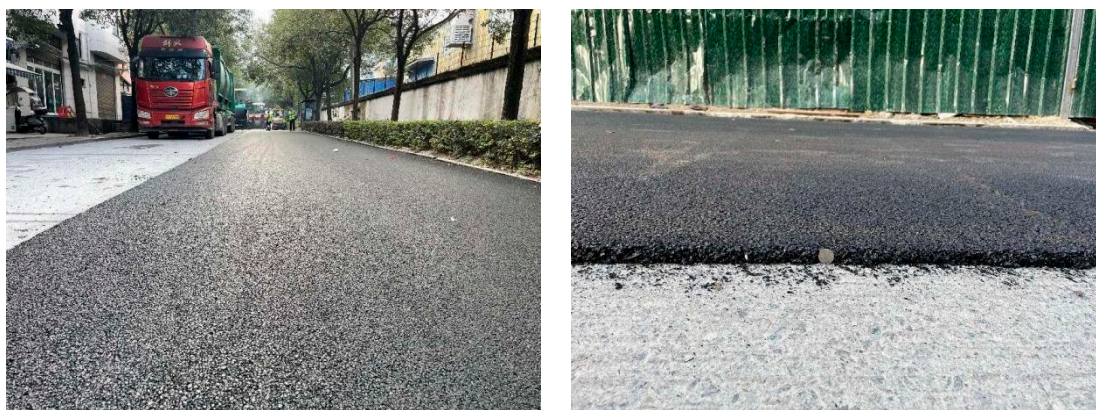


Figure 1. The maintenance sections of self-healing, ultra-thin overlay.

The fundamental properties of the materials used were measured according to the Chinese Standard of *Test Regulations for Asphalt and Asphalt Mixtures in Highway Engineering (JTG E20-2011)* [45]. Table 1 shows the fundamental properties of the SBS-modified asphalt binder, which was produced by Xiamen Huate Group Co., Ltd. (Xiamen, China). The basalt aggregate was provided by Fujian Zhangping Haoyuan Building Materials Co., Ltd. (Zhangping, China). Table 2 lists the basic properties for basalt aggregate. Meanwhile, a limestone powder provided by Fujian Sanyouxin Trading Co., Ltd. (Fuzhou, China) was used as the filler. To prepare the self-healing, ultra-thin overlay, this study used steel fiber as the conductive material for the self-healing induction due to its superior electromagnetic properties and durability in asphalt mixtures. The used steel fiber was provided by Jiangsu Jinjuoju Metal Products Co., Ltd. (Nantong, China) and had an average length of 4.2 mm;

the equivalent diameters ranged from 70 to 130 μm . The addition content of the steel fiber was 2.4% of mineral materials mass. Table 3 shows the fundamental mechanical properties of steel fiber. Figure 2 depicts the gradation curves for self-healing, ultra-thin asphalt overlay. According to the production proportions, the asphalt content for the asphalt mixture was 5.70% and the maximum theoretical density was 2.667 g/cm^3 .

Table 1. The fundamental properties of asphalt binder.

Tests	Units	Results	Test Methods
Penetration (25 °C, 100 g, 5 s)	0.1 mm	48	T0604-2011
Softening point	°C	84	T0606-2011
Ductility (5 cm/min, 5 °C)	cm	30	T0605-2011
Viscosity (135 °C)	Pa·s	1.23	T0625-2011
Density	g/cm^3	1.039	T0625-2011

Table 2. The fundamental properties of basalt aggregate.

Tests	Units	Results	Test Methods
Apparent relative density	g/cm^3	3.021	T0304-2005
Needle-like content	%	3.7	T0312-2005
Los Angeles wear and tear	%	7.4	T0317-2005
Crushing value	%	11.6	T0316-2005
Water absorption rate	%	0.81	T0304-2005

Table 3. The fundamental mechanical properties of steel fiber.

Tests	Units	Results
Density	g/cm^3	7.8
Oil content	%	<0.2
Equivalent diameter	μm	70–130
Average fiber length	mm	4.2
Melting point	°C	1530

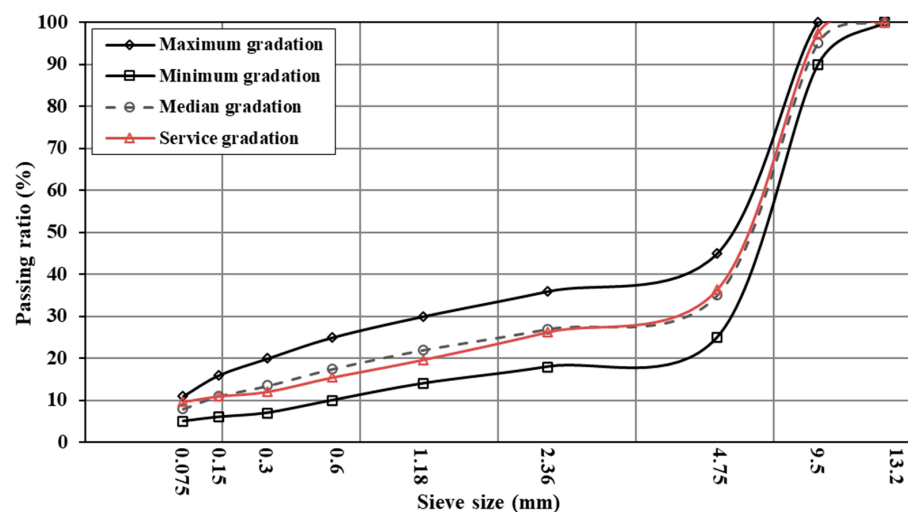


Figure 2. The gradation curves for self-healing, ultra-thin asphalt overlay.

2.2. Methods

2.2.1. Scope and Objectives

Asphalt pavement maintenance projects are accustomed to considering the environmental impacts and basic cost investment before implementing the practical works. Via the test section of the maintenance case, this comparative study will quantify the carbon emissions and economic costs of self-healing, ultra-thin overlay (SH overlay) and traditional overlay (TR overlay) by the methodology of life-cycle assessment (LCA) and life-cycle cost analysis (LCCA). The quantifying assessments will involve the carbon emissions and financial expenditures from material production and energy resource consumption, while the labor, agency services, and equipment procurement have not been considered, and neither have the negative impacts of traffic vehicles in the maintenance area. Moreover, the prepared asphalt mixture for the self-healing, ultra-thin overlay conformed to the road servicing requirements. From the case study, the comparative results could verify the environmental and economic benefits of self-healing, ultra-thin overlay and provide a significant reference for project managers in terms of balancing maintenance plans and further works.

2.2.2. System Boundary

According to the life cycle of ultra-thin overlay, there are four critical phases for the carbon emission assessments and economic cost analysis, and these include material extraction, on-site construction, later maintenance, and demolition. Figure 3 illustrates the system boundary for the SH overlay and TR overlay. To clarify the comparative benefits during the overlay’s life cycle, this study conducted the assessments using a functional unit with a length of 1 km and width of 3.75 m (single traffic lane). The compacted depth for the SH overlay and TR overlay were considered to be 20 mm and 40 mm, respectively. In addition, the later maintenance plans for the SH overlay and TR overlay were developed individually. Considering the six-year servicing period, it was assumed that induction heating cycles were carried out three times for the SH overlay in the second year, fourth year, and fifth year, respectively, and then the asphalt mixture was milled for demolition in the sixth year. Comparatively, the TR overlay would undergo the processes of milling and repaving the overlay in the third year and be demolished in the sixth year.

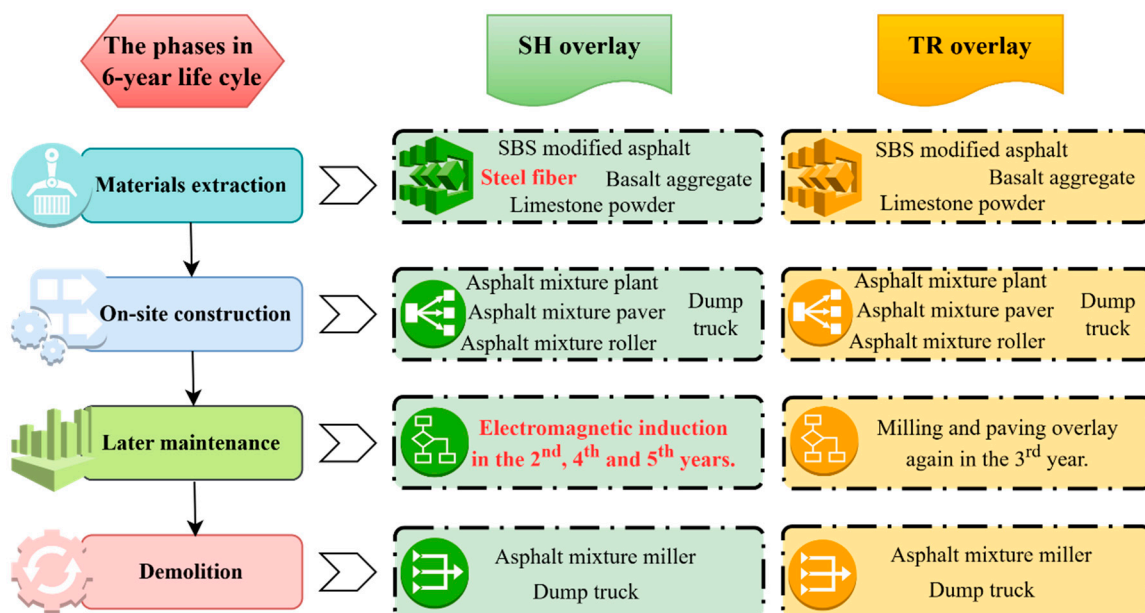


Figure 3. Research boundaries for the assessment of maintenance works.

2.2.3. Inventory Analysis

Via investigations from the practical maintenance project and the published literature, this study established a basic data inventory to quantify the integrative assessments. Table 4 shows the unit environmental impacts of material extraction and associated reference sources and demonstrates that the production of steel fiber would generate critical environmental burdens. Table 5 lists the unit calories and emission factors of energy resources based on *The 2006 IPCC Guidelines for National Greenhouse Gas Inventories* [46]. As for the economic costs of the maintenance case, this study integrated the market prices of materials and energy resources in Fujian Province in April 2023 from related suppliers and project reports, as shown in Tables 6 and 7, respectively. It should be noted that the market prices of materials exclude taxes and manual loading and unloading fees. Meanwhile, the prices of applied materials and energy resources may differ with time; hence, the quantified results for costs are only practical for the given period of time.

Table 4. Unit calorific value and carbon emissions of material extraction.

Materials	Unit Calories [MJ/t]	Unit Emission Factors [kg/t]	References
Base asphalt	2700.00	180.00	[47]
SBS-modified asphalt	7937.00	366.00	[48]
Steel fiber	6423.41	1973.28	[38]
Crushed aggregate	16.00	1.42	[49]
Mineral powder	38.00	2.57	[49]

Table 5. Unit calories and emissions of common energy sources.

Energy Type	Standard Coal Coefficients	Unit Calories	Unit Emission Factors
Coal	1.00	29.31 MJ/kg	2.70 kg/kg
Diesel	1.46	42.65 MJ/kg	3.31 kg/kg
Gasoline	1.47	43.07 MJ/kg	3.15 kg/kg
Heavy oil	1.43	41.82 MJ/kg	3.15 kg/kg
Electricity	0.12 kg/kWh	3.60 MJ/kWh	0.93 kg/kWh

Table 6. Reference market prices of common materials for the maintenance case.

Materials	Suppliers	Prices (CNY/t)
Base asphalt	Xiamen Huate Group Co., Ltd.	4800
SBS-modified asphalt	Xiamen Huate Group Co., Ltd.	5600
Basalt	Zhangping Haoyuan Building Materials Co., Ltd.	245
Limestone powder	Fujian Sanyouxin Trading Co., Ltd.	190
Steel fiber	Jiangsu Jinjuoju Metal Products Co., Ltd.	6200

Table 7. The considered market prices for energy resources.

Energy Sources	Market Prices	Units	Comments
92 octane gasoline	7.64	CNY/L	Market price
95 octane gasoline	8.15	CNY/L	Market price
Diesel	7.33	CNY/L	Market price
Heavy oil	5100.00	CNY/t	Market price
Industrial electricity	0.5959	CNY/kWh	Not exceeding 1 kV
	0.5759	CNY/kWh	1–10 kV
	0.5559	CNY/kWh	10–35 kV

To verify the assessments from the overlay maintenance project, Equations (1) and (2) demonstrate the basic principles for carbon emissions and economic costs from the material production processes, respectively. Meanwhile, Equations (3) and (4) show the associated principles of emissions and costs for energy resource consumption for mechanical works, respectively. As for the electromagnetic induction for the SH overlay, this study calculates the calorie values of induction heating according to the specific heat capacity and increasing temperature difference of asphalt material, as shown in Equation (5). It then transfers the calorie value to carbon emissions (Equation (6)) and economic costs (Equation (7)) with the associated energy resources. It is assumed that the induction heating operation would heat the asphalt from room temperature (25 °C) to 95 °C, and the specific heat capacity of asphalt was considered to be 1550 J/(kg * °C).

$$E_m = \sum_1^n (m_{im} \times e_{im}) \quad (1)$$

$$C_m = \sum_1^n (m_{im} \times c_{im}) \quad (2)$$

where E_m and C_m indicate the equivalent CO₂ emissions and economic costs of material production, respectively; m_{im} represents the total amount required for the material, i ; while e_{im} and c_{im} represent the equivalent CO₂ and the market price for producing the unit mass of material i , respectively.

$$E_e = \sum_1^n (m_{ie} \times e_{ie}) \quad (3)$$

$$C_e = \sum_1^n (m_{ie} \times c_{ie}) \quad (4)$$

where E_p and C_p represent the equivalent CO₂ emissions and economic costs from energy resource consumption, respectively; m_{ie} indicates the amount of fossil energy consumed by specific mechanical work i ; while e_{ie} and c_{ie} represent the equivalent CO₂ and market price generated by a unit mass of fossil energy, respectively.

$$CA = \alpha \times c \times \Delta t \times m \quad (5)$$

$$E_{sh} = \frac{CA}{C_0} \times e_{ie} \quad (6)$$

$$C_{sh} = \frac{CA}{C_0} \times c_{ie} \quad (7)$$

where CA is the calorie value of electromagnetic induction works and α is the effective thermal conductivity, which was assumed to be 50% in this study; c stands for the specific heat capacity of asphalt; Δt is the increased temperature; E_{sh} and C_{sh} represent the equivalent CO₂ emissions and economic costs from induction works, respectively; and C_0 is the unit calorie of the energy resource i , while e_{ish} and c_{ish} represent the equivalent CO₂ and market price generated by a unit mass of energy resource i , respectively.

3. Results and Discussions

3.1. Comparative Assessments for Materials Extractions

Figure 4 shows the carbon emissions of SH overlay and TR overlay during the material extraction phase. Although the materials required for the SH overlay were only half that of the TR overlay, the overall emissions from the material extraction phase was still higher than that of the TR overlay. The material production and transport of SH overlay caused 14,594.05 kg of equivalent CO₂, and the emissions by the TR overlay reached 11,682.12 kg of equivalent CO₂. According to the analysis of the emissions from different materials, the steel fiber generated the most carbon emissions, with 8741.99 kg of equivalent CO₂, although it had the lowest dosage (mass proportion of 2.21% in the asphalt mixture). The carbon emissions generated by SBS-modified asphalt also occupied a greater percentage. Specifically, the SBS-modified asphalt in SH overlay and TR overlay resulted in 4277.42 kg and 8523.64 kg of equivalent CO₂, respectively. Meanwhile, the emissions from crushed aggregate achieved 1433.46 kg and 2780.87 kg in the SH overlay and TR overlay, respectively. Additionally, acquiring the mineral powder released the least carbon emissions, with 141.18 kg for the SH overlay and 377.61 kg for the TR overlay.

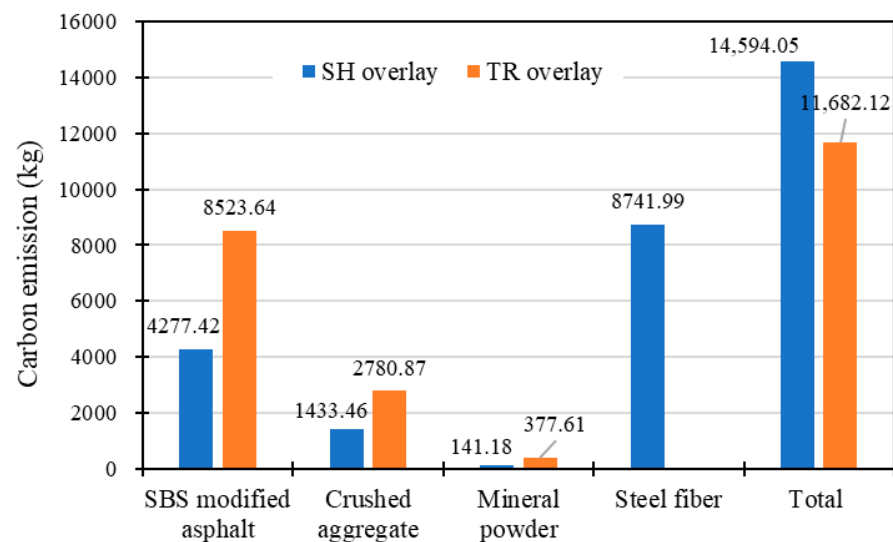


Figure 4. Carbon emissions for the material extraction phase.

Figure 5 demonstrates the economic costs of SH overlay and TR overlay during the material extraction phase. The results show that the TR overlay resulted in an economic cost of CNY 220,536.10, which was CNY 82,401.04 more than the SH overlay. Among the materials, SBS-modified asphalt released the most carbon emissions, with CNY 125,303.35 in the TR overlay and CNY 62,880.51 in the SH overlay. Purchasing crushed aggregate lead to the second largest cost, with CNY 86,080.96 in the TR overlay and CNY 44,372.43 in the SH overlay. For the SH overlay, the limited addition of steel fiber led to its cost being CNY 27,460.25 under the functional unit, even though the unit market price of steel fiber was high. Comparing the other materials, the limestone powder had the least economic cost for both the SH overlay and the TR overlay, which resulted in costs of CNY 3421.88 and CNY 9152.79 for the functional unit, respectively.

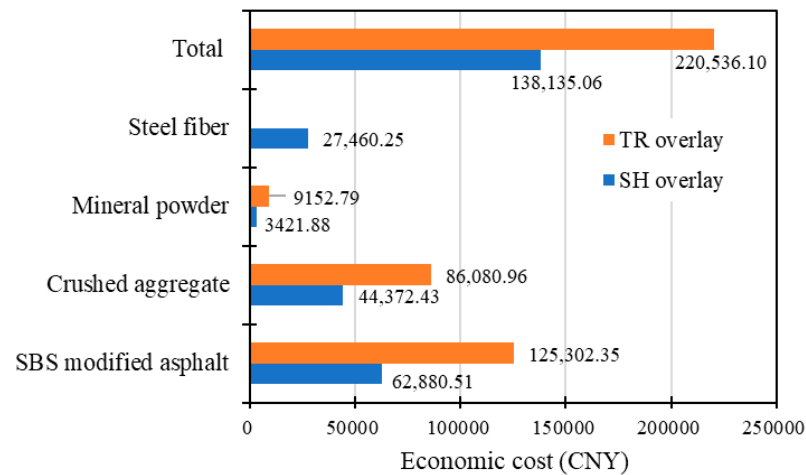


Figure 5. Economic costs for the material extraction phase.

3.2. Comparative Assessments for On-Site Construction

Figure 6 demonstrates the comparative carbon emissions for the on-site works of the SH overlay and the TR overlay, which involved the asphalt mixture preparation, asphalt mixture transport, asphalt mixture paving and milling, and tack coat spraying. Among these, preparing the asphalt mixture caused the most carbon emissions, with 6603.57 kg of equivalent CO₂ for the SH overlay and 13,032.37 kg of equivalent CO₂ for the TR overlay, because preheating the aggregate and asphalt binder consumes massive energy resources. However, the carbon emissions from the asphalt mixture transport, asphalt mixture paving and milling, and tack coat spraying were evidently less than the asphalt mixture preparation, fluctuating from 400 to 700 kg of equivalent CO₂ for the SH overlay and 600 to 900 kg of equivalent CO₂ for the TR overlay. Generally, the construction works of the TR overlay emitted 15,305.14 kg of equivalent CO₂, which was 7109.87 kg more than that of the SH overlay.

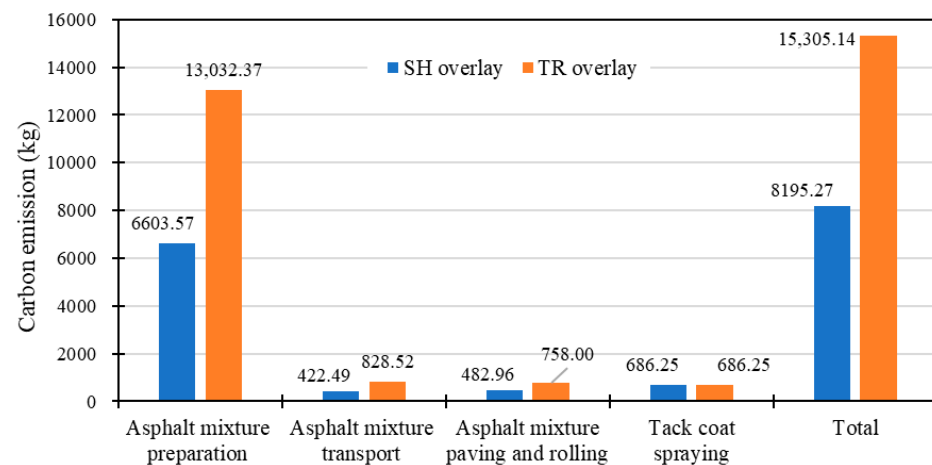


Figure 6. Carbon emissions for the on-site construction phase.

Figure 7 shows the economic costs of on-site construction works for the SH overlay and the TR overlay. Varying from the results of carbon emissions in Figure 6, spraying the tack coat consumed the most economic cost, with CNY 11,437.05 in both the SH overlay and the TR overlay, because the cost of purchasing tack coat was also considered in the process. Preparation of the asphalt mixture became the second-highest cost generator, with CNY 7428.12 in the SH overlay and CNY 3763.87 in the TR overlay. The energy resource consumption for asphalt mixture transport and on-site machinery (paver and rollers) were similar; hence, their costs differed only slightly in both the SH overlay and the

TR overlay. The total costs for the SH overlay and the TR overlay were CNY 17,344.48 and CNY 22,631.20 in the on-site construction phase, respectively.

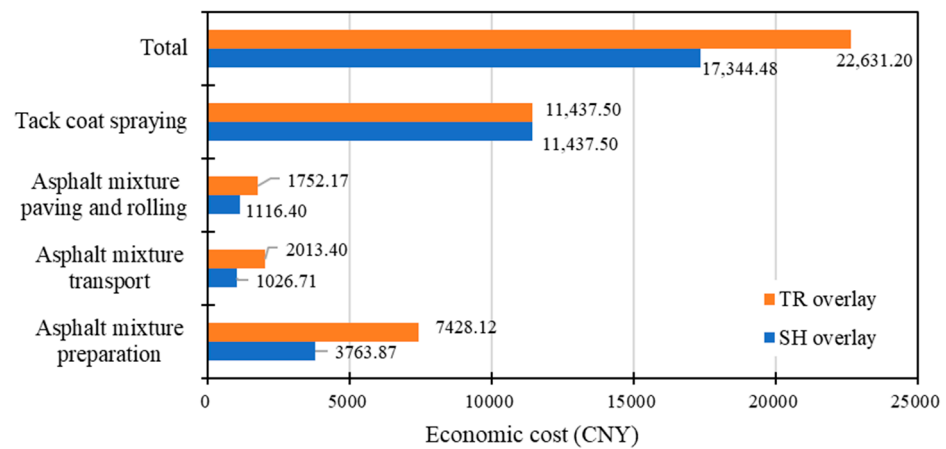


Figure 7. Economic costs for the on-site construction phase.

3.3. Comparative Assessments for Later Maintenance

The primary benefits of self-healing technology is reflected in the later maintenance phase for ultra-thin overlay. Figure 8a,b exhibit the carbon emissions and economic costs of the SH overlay and TR overlay, respectively. In the second, fourth, and fifth years, conducting the electromagnetic induction operations would lead to 793.83 kg of equivalent CO₂ each time, and the associated costs were CNY 527.33. For the later maintenance of the TR overlay, implementing the works of milling the aged layer and repaving the fresh overlay would result in carbon emissions of 36,016.56 kg of equivalent CO₂ in the third year, and the financial cost reached CNY 349,986.09. Comparatively, the three instances of induction heating operation generated 2381.49 kg of equivalent CO₂ for the SH overlay, which was only 6.61% of the emissions from the TR overlay in the later maintenance phase, and the cumulative cost over three years accounted for less than 1% of the latter, with CNY 1581.99. Therefore, significant benefits were shown for the SH overlay in the later maintenance phase.

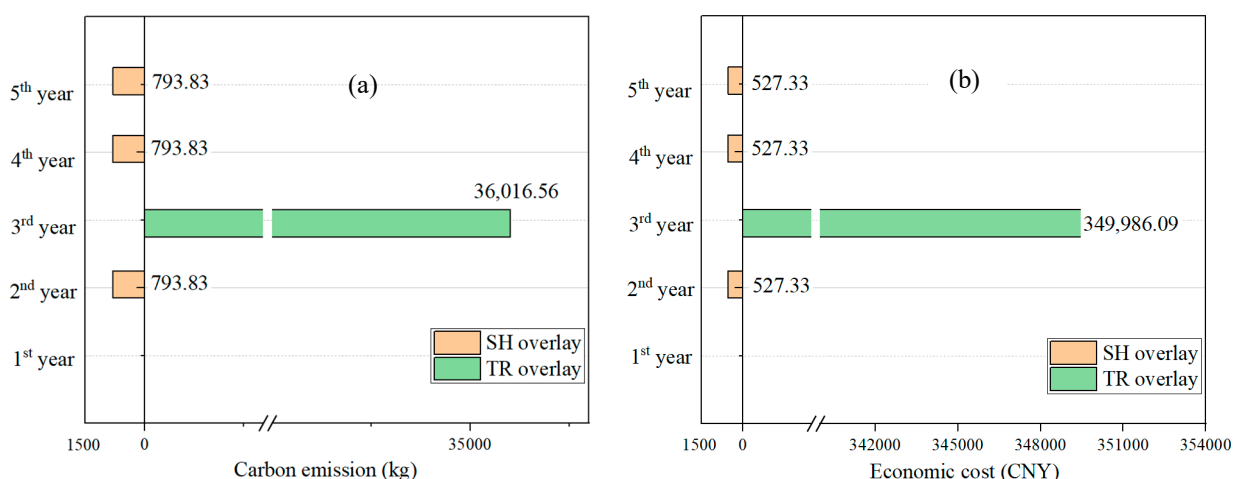


Figure 8. (a) Carbon emissions and (b) economic costs for the later maintenance phase.

3.4. Comparative Assessments for Demolition

The demolition phase mainly consists of the milling and transportation of aged asphalt mixture. Figure 9a,b illustrate the carbon emissions and economic costs of SH overlay and TR overlay, respectively. Due to the differences in structural thickness, there would be twice

the workload for the TR overlay than for the SH overlay in both milling and transportation. Specifically, milling the overlay led to 1623.78 kg and 3063.73 kg of equivalent CO₂ for the SH overlay and the TR overlay, respectively, and the corresponding costs were CNY 4390.37 and CNY 8283.72. Moreover, the impacts of transporting RAP only occupied approximately 2% of the milling works in both the SH overlay and the TR overlay. The total carbon emissions and economic costs of the SH overlay were 1657.61 kg of equivalent CO₂ and CNY 4481.84, and 3127.56 kg of equivalent CO₂ and CNY 8456.30 for the TR overlay.

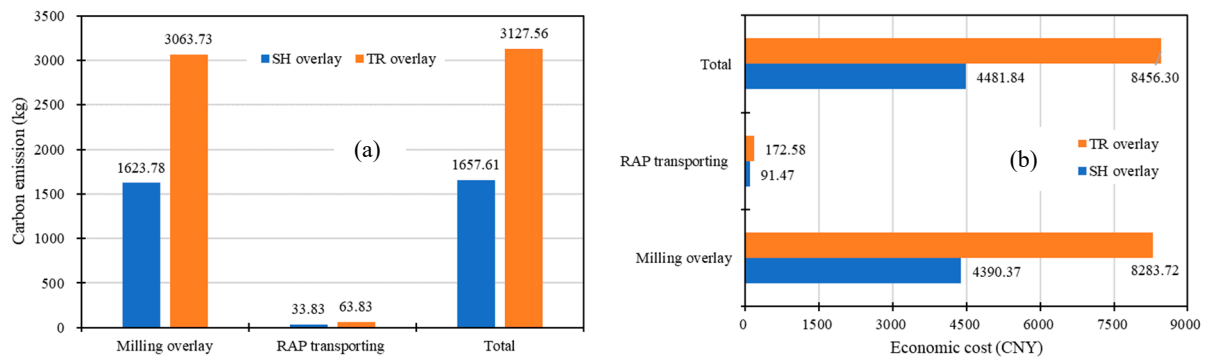


Figure 9. (a) Carbon emissions and (b) economic costs for the demolition phase.

3.5. Integrative Profits for Life-Cycle Carbon Emissions and Costs

This study investigated the integrative profits for SH overlay and TR overlay over a six-year life span. Partial results were exhibited in Figure 10a,b, which summarize the carbon emissions and associated percentages for different phases, respectively. In the life cycle, the SH overlay could reduce carbon emissions by 39,302.95 kg of equivalent CO₂ within the functional unit. Compared with the carbon emissions of critical phases, the material extraction phase in the SH overlay surpassed the TR overlay by 2911.93 kg of equivalent CO₂, while all the other three phases were lower than the latter. Especially in the later maintenance phase, significant environment benefits were obtained for the SH overlay. Considering the distribution percentages of the critical phases in the SH overlay, the material extraction phase and on-site construction phase resulted in 54% and 31% of carbon emission, respectively, but both the later maintenance phase and demolition phase were less than 10%. For the TR overlay, the highest carbon emissions were from the later maintenance phase, with a percentage of 54%, while the on-site construction phase and material extraction phase caused 23% and 18% of carbon emission, respectively.

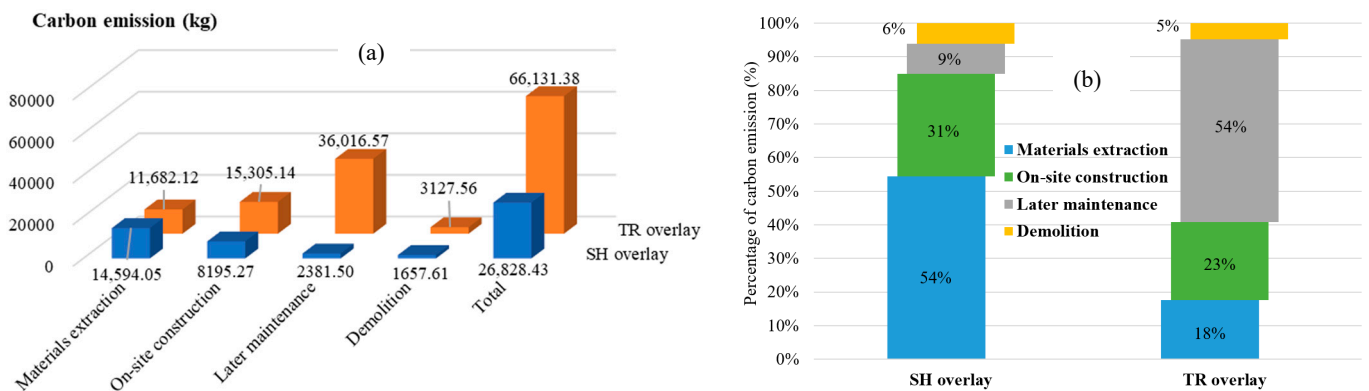


Figure 10. Life cycle (a) carbon emissions and (b) distribution percentages.

Figure 11a,b show the economic costs and distribution percentages of the SH overlay and TR overlay, respectively. In the functional unit with a six-year life span, the SH overlay

could save 73.15% of the economic costs of the TR overlay, with costs of CNY 161,543.37. The economic costs of the TR overlay exceeded those of the SH overlay in all four critical phases, and the highest difference in cost value appeared in the later maintenance phase. As for the distribution percentages of critical phases in the life cycle, the material extraction phase was the greatest economic consumer for the SH overlay by 85% of the total economic cost, and the later maintenance phase had the least cost, by 1% of the total. But for the TR overlay, the largest economic cost was generated in the later maintenance phase, and the on-site construction phase and demolition phase were minimal, resulting in 4% and 1% of the total economic cost, respectively.

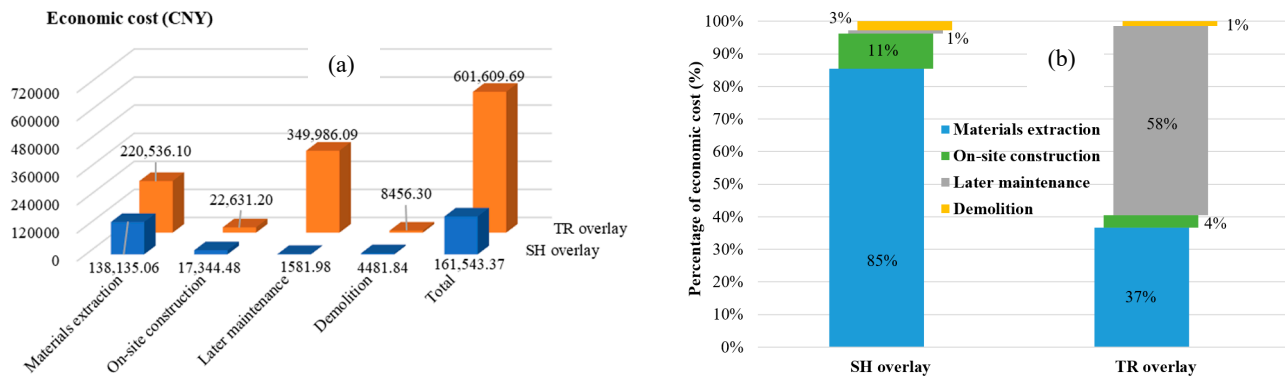


Figure 11. Life cycle (a) economic costs and (b) distribution percentages.

4. Conclusions

This study conducted a comparative analysis to cover the gap in quantifying the environmental impacts and economic costs of self-healing, ultra-thin overlay. The fundamental properties of steel fiber were tested and utilized in the ultra-thin overlay for induction healing capacity. Moreover, the system framework of self-healing, ultra-thin overlay was developed toward the six-year life cycle, involved in the materials extraction, on-site construction, later maintenance and demolition phases. Meanwhile, the primary data inventories for both carbon emissions and economic cost were established according to the investigation for the test section of maintenance project. Through analyzing the quantitative results for self-healing, ultra-thin overlay and traditional overlay in life cycle, several conclusions can be drawn below.

- (1) In the six-year life cycle of overlay maintenance, applying self-healing, ultra-thin overlay could reduce 59.43% of carbon emissions and 73.15% of economic costs.
- (2) The material extraction phase generated over 50% of carbon emissions and economic costs in self-healing, ultra-thin overlay, while for traditional thin overlay, the later maintenance phase resulted in the over half of carbon emissions and costs.
- (3) The addition of steel fiber would rise the burdens in material extraction phase for self-healing, ultra-thin overlay, but the later maintenance by induction heating sharply decreased overall carbon emissions and economic costs.

Author Contributions: F.W.: Conceptualization, Investigation, Writing-original draft. X.L.: Supervision, Conceptualization, Investigation. C.H.: Conceptualization, Investigation, Writing-review & editing. W.Z.: Investigation, Writing-review & editing. D.L.: Investigation, Writing-review & editing. All authors have read and agreed to the published version of the manuscript.

Funding: This study was funded by the State Key Laboratory of Silicate Materials for Architectures (Wuhan University of Technology) (SYSJJ2023-05), the China Postdoctoral Science Foundation (2023M731207), Fujian Provincial Transportation Technology Project (202261), Post-doctoral Innovation Research Positions of Hubei Province (0106242015), National Key R&D Program of China (No. 2018YFB1600200), Key R&D Program of Guangxi Province (No. 2021AB26023), National Natural Science Foundation of China (No. 51978547 and 52111530134), Key R&D Program of Hubei Province (No. 2020BCB064), Technological Innovation Major Project of Hubei Province (2019AEE023).

Data Availability Statement: The data presented in this study are available on request from the corresponding author.

Conflicts of Interest: The authors declare no conflict of interest.

References

- Hoy, M.; Samrandee, V.; Samrandee, W.; Suddeepong, A.; Phummiphan, I.; Horpibulsuk, S.; Buritatum, A.; Arulrajah, A.; Yeanyong, C. Evaluation of asphalt pavement maintenance using recycled asphalt pavement with asphalt binders. *Constr. Build. Mater.* **2023**, *406*, 133425. [\[CrossRef\]](#)
- Yao, L.; Leng, Z.; Ni, F.; Lu, G.; Jiang, J. Adaptive maintenance strategies to mitigate climate change impacts on asphalt pavements. *Transp. Res. Part D Transp. Environ.* **2024**, *126*, 104026. [\[CrossRef\]](#)
- Stuart, K.D. *Moisture Damage in Asphalt Mixtures—A State-of-the-Art Report*; United States. Federal Highway Administration. Office of Engineering and Highway Operations R&D: McLean, VA, USA, 1990.
- Chinese Ministry of Transport. *Statistical Bulletin on the Development of Transportation Industry in 2023*; Chinese Ministry of Transport: Beijing, China, 2024.
- Liu, G.; Zhang, X.; Qian, Z.; Chen, L.; Bi, Y. Life cycle assessment of road network infrastructure maintenance phase while considering traffic operation and environmental impact. *J. Clean. Prod.* **2023**, *422*, 138607. [\[CrossRef\]](#)
- Underwood, B.S.; Guido, Z.; Gudipudi, P.; Feinberg, Y. Increased costs to US pavement infrastructure from future temperature rise. *Nat. Clim. Change* **2017**, *7*, 704–707. [\[CrossRef\]](#)
- Huang, M.; Dong, Q.; Ni, F.; Wang, L. LCA and LCCA based multi-objective optimization of pavement maintenance. *J. Clean. Prod.* **2021**, *283*, 124583. [\[CrossRef\]](#)
- Zhu, Z.; Zhang, Y.; Wu, H.; Zhou, M. Assessment and Suggestions on Impact of Product Oil Tax and Fee Reform on Road Transport Development. *J. Highw. Transp. Res. Dev.* **2023**, *40*, 234–239.
- Rupasinghe, B.; Wallace, M.; Gange, G.; Senthoran, I. Road pavement upgrade scheduling accounting for minimizing congestion. *Sci. Rep.* **2023**, *13*, 15386. [\[CrossRef\]](#)
- Wang, H.; Wu, Z.; Wu, Z.; Hou, Q. Urban network noise control based on road grade optimization considering comprehensive traffic environment benefit. *J. Environ. Manag.* **2024**, *364*, 121451. [\[CrossRef\]](#)
- Zhang, J.; Gao, L.; Dong, Z. Review on Materials and Technology of Multifunctional Maintenance of Asphalt Pavement. *J. Munic. Technol.* **2023**, *41*, 80–93.
- Hajj, R.; Filonzi, A.; Smit, A.; Bhasin, A. Design and Performance of Mixes for Use as Ultrathin Overlay. *J. Transp. Eng. Part B Pavements* **2019**, *145*, 04019026. [\[CrossRef\]](#)
- Hong, B.; Lu, G.; Gao, J.; Dong, S.; Wang, D. Green tunnel pavement: Polyurethane ultra-thin friction course and its performance characterization. *J. Clean. Prod.* **2021**, *289*, 125131. [\[CrossRef\]](#)
- Guo, M.; Zhang, R.; Du, X.; Liu, P. A State-of-the-Art Review on the Functionality of Ultra-Thin Overlays Towards a Future Low Carbon Road Maintenance. *Engineering* **2024**, *32*, 82–98. [\[CrossRef\]](#)
- Yu, J.; Feng, Z.; Chen, Y.; Yu, H.; Korolev, E.; Obukhova, S.; Zou, G.; Zhang, Y. Investigation of cracking resistance of cold asphalt mixture designed for ultra-thin asphalt layer. *Constr. Build. Mater.* **2024**, *414*, 134941. [\[CrossRef\]](#)
- Song, W.; Zou, X.; Wu, H.; Zhou, L.; Zhou, Y. Fracture properties of ultra-thin friction course mixture containing reclaimed asphalt pavement and glass fiber under monotonic and cyclic loading. *Theor. Appl. Fract. Mech.* **2024**, *133*, 104595. [\[CrossRef\]](#)
- Chen, S.; Gong, F.; Ge, D.; You, Z.; Sousa, J.B. Use of reacted and activated rubber in ultra-thin hot mixture asphalt overlay for wet-freeze climates. *J. Clean. Prod.* **2019**, *232*, 369–378. [\[CrossRef\]](#)
- Wang, J.; Li, Q.; Song, G.; Luo, S.; Ge, D. Investigation on the comprehensive durability and interface properties of coloured ultra-thin pavement overlay. *Case Stud. Constr. Mater.* **2022**, *17*, e01341. [\[CrossRef\]](#)
- Usman, K.R.; Hainin, M.R.; Idham, M.K.; Warid, M.N.M.; Yaacob, H.; Hassan, N.A.; Azman, M.; Puan, O.C. Performance evaluation of asphalt micro surfacing—A review. *IOP Conf. Ser. Mater. Sci. Eng.* **2019**, *527*, 012052. [\[CrossRef\]](#)
- Ding, L.; Wang, X.; Zhang, K.; Zhang, M.; Yang, J.; Chen, Z. Durability evaluation of easy compaction and high-durability ultra-thin overlay. *Constr. Build. Mater.* **2021**, *302*, 124407. [\[CrossRef\]](#)
- Liu, Z.; Wang, X.; Luo, S.; Yang, X.; Li, Q. Asphalt mixture design for porous ultra-thin overlay. *Constr. Build. Mater.* **2019**, *217*, 251–264. [\[CrossRef\]](#)
- Yu, J.; Chen, F.; Deng, W.; Ma, Y.; Yu, H. Design and performance of high-toughness ultra-thin friction course in south China. *Constr. Build. Mater.* **2020**, *246*, 118508. [\[CrossRef\]](#)
- Bazin, P.; Saunier, J. Deformability, Fatigue and healing properties of asphalt mixes. In Proceedings of the International Conference on the Structural Design of Asphalt Pavements, Ann Arbor, MI, USA, 7–11 August 1967; pp. 438–451.
- Xu, S.; García, A.; Su, J.; Liu, Q.; Tabaković, A.; Schlangen, E. Self-Healing Asphalt Review: From Idea to Practice. *Adv. Mater. Interfaces* **2018**, *5*, 1800536. [\[CrossRef\]](#)
- García, Á.; Schlangen, E.; van de Ven, M.; Liu, Q. Electrical conductivity of asphalt mortar containing conductive fibers and fillers. *Constr. Build. Mater.* **2009**, *23*, 3175–3181. [\[CrossRef\]](#)
- Liu, Q.; Schlangen, E.; García, Á.; van de Ven, M. Induction heating of electrically conductive porous asphalt concrete. *Constr. Build. Mater.* **2010**, *24*, 1207–1213. [\[CrossRef\]](#)

27. Wan, P.; Wu, S.; Liu, Q.; Wang, H.; Gong, X.; Zhao, Z.; Xu, S.; Jiang, J.; Fan, L.; Tu, L. Extrinsic self-healing asphalt materials: A mini review. *J. Clean. Prod.* **2023**, *425*, 138910. [[CrossRef](#)]
28. Yang, C.; Wu, S.; Xie, J.; Amirkhanian, S.; Liu, Q.; Zhang, J.; Xiao, Y.; Zhao, Z.; Xu, H.; Li, N.; et al. Enhanced induction heating and self-healing performance of recycled asphalt mixtures by incorporating steel slag. *J. Clean. Prod.* **2022**, *366*, 132999. [[CrossRef](#)]
29. Ye, X.; Chen, Y.; Yang, H.; Xiang, Y.; Ye, Z.; Li, W.; Hu, C. Enhancing self-healing of asphalt mixtures containing recycled concrete aggregates and reclaimed asphalt pavement using induction heating. *Constr. Build. Mater.* **2024**, *439*, 137361. [[CrossRef](#)]
30. Ye, X.; Li, X.; Chen, Y.; Yang, H.; Xiang, Y.; Ye, Z.; Hu, C. Optimum moment to heal cracks in asphalt pavement by means of waste carbon fiber-enhanced electromagnetic induction heating during multiple damage-healing cycles. *J. Clean. Prod.* **2024**, *470*, 143265. [[CrossRef](#)]
31. Li, J.; Gao, M.; Li, X. Study on the Influence of Steel Slag and Steel Fiber on Microwave Heating Properties of Asphalt Mixture. *J. Munic. Technol.* **2024**, *42*, 256–262.
32. Jiao, W.; Sha, A.; Liu, Z.; Jiang, W.; Hu, L.; Li, X. Utilization of steel slags to produce thermal conductive asphalt concretes for snow melting pavements. *J. Clean. Prod.* **2020**, *261*, 121197. [[CrossRef](#)]
33. Liu, K.; Zhang, H.; Da, Y.; Wang, F.; Liu, Q. Regulatory strategy for balancing deicing efficiency and energy-saving effects of induction heating asphalt pavements. *J. Clean. Prod.* **2024**, *466*, 142812. [[CrossRef](#)]
34. Wang, J.; Feng, K.; Feng, J.; Yao, S.; Dong, W. Review of Construction and Maintenance of Carbon Emission and Low-carbon Path of Asphalt Pavement. *J. Munic. Technol.* **2024**, *42*, 55–60.
35. Lizasoain-Arteaga, E.; Indacochea-Vega, I.; Pascual-Muñoz, P.; Castro-Fresno, D. Environmental impact assessment of induction-healed asphalt mixtures. *J. Clean. Prod.* **2019**, *208*, 1546–1556. [[CrossRef](#)]
36. Rodríguez-Alloza, A.M.; Heihsel, M.; Fry, J.; Gallego, J.; Geschke, A.; Wood, R.; Lenzen, M. Consequences of long-term infrastructure decisions—The case of self-healing roads and their CO₂ emissions. *Environ. Res. Lett.* **2019**, *14*, 114040. [[CrossRef](#)]
37. Liu, J.; Jing, H.; Wang, Z.; Wang, X.; Zhang, L. Recycling of steel slag in sustainable bituminous mixtures: Self-healing performance, mechanism, environmental and economic analyses. *J. Clean. Prod.* **2023**, *429*, 139496. [[CrossRef](#)]
38. Wang, F.; Hoff, I.; Yang, F.; Wu, S.; Xie, J.; Li, N.; Zhang, L. Comparative assessments for environmental impacts from three advanced asphalt pavement construction cases. *J. Clean. Prod.* **2021**, *297*, 126659. [[CrossRef](#)]
39. Wan, J.; Xiao, Y.; Song, W.; Chen, C.; Pan, P.; Zhang, D. Self-Healing Property of Ultra-Thin Wearing Courses by Induction Heating. *Materials* **2018**, *11*, 1392. [[CrossRef](#)] [[PubMed](#)]
40. Wan, J.; Wu, S.; Xiao, Y.; Fang, M.; Song, W.; Pan, P.; Zhang, D. Enhanced ice and snow melting efficiency of steel slag based ultra-thin friction courses with steel fiber. *J. Clean. Prod.* **2019**, *236*, 117613. [[CrossRef](#)]
41. Liu, W.; Wan, P.; Wu, S.; Liu, Q.; Wang, J.; Jiang, Q.; Xu, H. Effect of aging level on the healing properties of an induction-heated ultra-thin wearing course and its mechanism. *Constr. Build. Mater.* **2024**, *430*, 136506. [[CrossRef](#)]
42. Xu, H.; Wu, S.; Chen, A.; Zou, Y.; Yang, C.; Cui, P. Study on preparation and characterization of a functional porous ultra-thin friction course (PUFC) with recycled steel slag as aggregate. *J. Clean. Prod.* **2022**, *380*, 134983. [[CrossRef](#)]
43. Hoxha, E.; Vignisdottir, H.R.; Barbieri, D.M.; Wang, F.; Bohne, R.A.; Kristensen, T.; Passer, A. Life cycle assessment of roads: Exploring research trends and harmonization challenges. *Sci. Total Environ.* **2021**, *759*, 143506. [[CrossRef](#)]
44. Wang, F.; Xie, J.; Wu, S.; Li, J.; Barbieri, D.M.; Zhang, L. Life cycle energy consumption by roads and associated interpretative analysis of sustainable policies. *Renew. Sustain. Energy Rev.* **2021**, *141*, 110823. [[CrossRef](#)]
45. *JTG E20-2011*; Chinese Ministry of Transport, Test Regulations for Asphalt and Asphalt Mixtures in Highway Engineering. Chinese Ministry of Transport: Beijing, China, 2011.
46. Eggleston, H.; Buendia, L.; Miwa, K.; Ngara, T.; Tanabe, K. *2006 IPCC Guidelines for National Greenhouse Gas Inventories*; The Institute for Global Environmental Strategies (IGES): Hayama, Kanagawa, 2006.
47. Giani, M.I.; Dotelli, G.; Brandini, N.; Zampori, L. Comparative life cycle assessment of asphalt pavements using reclaimed asphalt, warm mix technology and cold in-place recycling. *Resour. Conserv. Recycl.* **2015**, *104*, 224–238. [[CrossRef](#)]
48. Wang, F.; Li, X.; Wu, S.; Zheng, L.; Luo, Q.; Zhang, J.; Barbieri, D.M. Comparative study for global warming potentials of Chinese and Norwegian roads with life cycle assessment. *Process Saf. Environ. Prot.* **2023**, *177*, 1168–1180. [[CrossRef](#)]
49. Ozelik, M. Energy consumption analysis for natural aggregate processing and its results (Atabey, Isparta, Turkey). *Min. Miner. Depos.* **2018**, *12*, 80–86. [[CrossRef](#)]

Disclaimer/Publisher’s Note: The statements, opinions and data contained in all publications are solely those of the individual author(s) and contributor(s) and not of MDPI and/or the editor(s). MDPI and/or the editor(s) disclaim responsibility for any injury to people or property resulting from any ideas, methods, instructions or products referred to in the content.